

# Tactile Servo Using Dynamic Tactile Jacobian Estimator

Chen-Ting Wen, Jun Kinugawa, Shogo Arai and Kazuhiro Kosuge

*Graduate School of Engineering, Department of Robotics  
 Tohoku University*

6-6-01, Aramaki Aza-Aoba, Aoba ward, Sendai, Miyagi. 980-8579, Japan

{wen.chen.ting.r4}@dc.tohoku.ac.jp, {kinugawa, arai, kosuge}@tohoku.ac.jp

**Abstract**—Nowadays, a wide variety of service robots have been developed to assist humans in performing tasks that are dull and repetitive, such as household chores. Tactile perception can play a critical role in a service robot to improve its performance. Thus, the robot control method with tactile perception, Tactile servo, was proposed. However, the common tactile servo cannot deal with the targets so generally and flexibly. To enhance the performance of the tactile servo, this study is to present an agile and versatile tactile servo by the dynamic tactile Jacobian estimator which can generate an adjustable tactile Jacobian instead of a fixed tactile Jacobian used in the common tactile servo. In the experimental validation, this research utilized the objects with different shapes for experimenting, and this research confirmed the feasibility of the tactile servo using the dynamic tactile Jacobian estimator in final. This paper explains the method and demonstrates the results.

**Index Terms**—tactile servo, tactile Jacobian estimator, pressure distribution

## I. INTRODUCTION

Over the past few years, a wide variety of service robots[1][2] have been proposed and developed to perform tasks that are dull and repetitive including household chores, such as part classification[3], object positioning[4], and human interaction[5]-[9]. Because the service robots have to physically interact, such as touch, with their surroundings, most of them adopt the tactile sensors to be a method for observing[10][11] and interacting[12] with their surroundings. Even if a robot with visual sensors wants to have a much more precise detail of surroundings and targets, the cooperation with the tactile sensation is a common method to deal with the acquisition of a lack of information about the target. Therefore, we learn the tactile sensation is also an essential function for a service robot to measure its surroundings.

The service robots are usually designed with tactile sensation to perform the various tasks in their surroundings. However, the environment is complicated, and every contacting object has its unique appearance, such as a curved surface or an irregular surface. Thus, the criterion of safe interaction between a robot and the different objects, such as contacting an object or touching a human, is also not the same. How to use the tactile sensation for a service robot to deal with the tasks and have a dexterous and safe behavior simultaneously is a critical issue.

Tactile servo is a common robot control method by tactile sensation to deal with the issues about robot interaction. However, each current tactile servo can only apply to contact

the specified surface on the target to perform tasks. Thus, it is not so general and flexible. For a service robot, these tactile servo cannot attain the requirement of dexterous and safe interaction with its surroundings. We want to have a new control scheme for tactile servo to be more agile and general. The objective of this study was to provide an adjustable and versatile tactile servo to enable the robot to be able to contact the unknown target without any prior information about the appearance of the target.

## II. BACKGROUND AND RELATED WORKS

Tactile sensing array[13][14], which is one kind of tactile sensor, can endow a robot with the tactile sensation[15]. Due to the superior performance on the spatial resolution of the tactile sensing array, in which the robot equipped can perceive the information of surroundings by touch[16][17]. The robot cannot just feel, and it can even operate an object by the feedback of tactile sensation[18][19]. Consequently, tactile servo was proposed for robot control[20].

Tactile servo[21][22] is a control method for a robot to interact with its surroundings in a proper motion[23][24]. The control scheme depicts in Fig.1. While the robot is contacting or operating an object, its tactile sensing array presents the observed tactile information. And then, the tactile features are extracted from the observed the tactile information by feature extraction. Consequently, the deviation of the desired and extracted tactile features are utilized to generate the input for the robot through tactile Jacobian.

Fig.1 shows tactile Jacobian plays a crucial role in tactile servo. Tactile Jacobian can provide a proper robot motion by the input of difference in tactile information so that the tactile servo has a proper performance. The previous researches[20]-[24] obtained the fixed tactile Jacobian by the least-squares method, the robotic displacement, and the corresponding tactile features. However, the conventional tactile servo with the fixed tactile Jacobian can only operate in the specified region, which is the area for acquiring the robot movement and the tactile

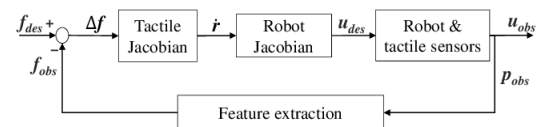


Fig. 1. Tactile servo: the robot can perform a robot motion  $\mathbf{u}_{des}$  through the deviations of tactile features  $\Delta \mathbf{f}$  by feature extraction from pressure distribution  $\mathbf{p}_{obs}$ .

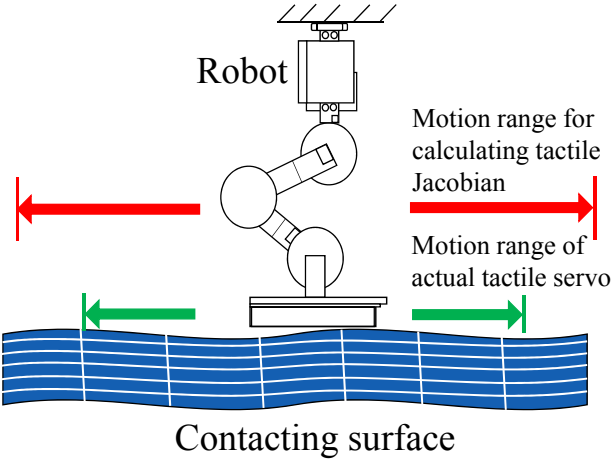


Fig. 2. Range of robot motion by the conventional tactile servo. The red arrow is the range for the robot to obtain robot motion and the corresponding tactile information for the tactile Jacobian. The green arrow represents the real available range for the robot with the fixed tactile Jacobian.

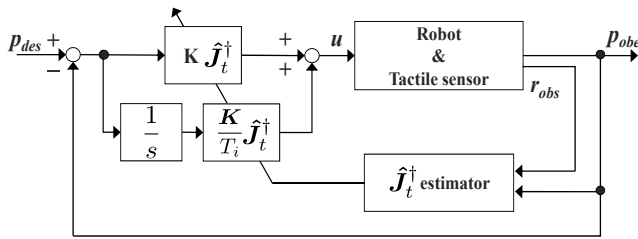


Fig. 3. Block diagram of tactile servo.  $\hat{\mathbf{J}}_t^\dagger$  can be obtained by the error between the desired pressure distribution  $\mathbf{p}_{des}$  and the observed pressure distribution  $\mathbf{p}_{obe}$ . The PI controller is able to generate the input  $u$  for the robot.

features to calculate tactile Jacobian (see Fig.2). Thus, if the robot with the conventional tactile servo wants to attain the purpose of this study, the preparation of tactile Jacobian to fit the several different surfaces is essential.

In this paper, we present a new method of estimating tactile Jacobian to increase the multi-usability of tactile servo. The characteristic of this method is to utilize a dynamic estimation of tactile Jacobian instead of a fixed tactile Jacobian to fit the different contact surfaces flexibly. This paper contributes to provide a versatile and dexterous estimator to calculate tactile Jacobian for tactile servo. In the following content of this paper, we explain and demonstrate a tactile servo with a dynamic tactile Jacobian estimator.

### III. ESTIMATION OF TACTILE JACOBIAN

#### A. Tactile Features and Controller of Tactile Servo

The structure of tactile servo is analogous to image-based visual servo using eye-in-hand[21], and image Jacobian in visual servo is the bridge to connect the velocity of a visual sensor and the pixel's changing. In tactile servo, tactile Jacobian plays an identical role for tactile servo. By the inspiration of concept, the method of dynamic tactile Jacobian is similar to visual Jacobian.

For tactile servo, the utilization of tactile information is important. The different tactile features have different char-

acteristics on the performance of tactile servo. To have a clear and precise tactile information, the utilization of pressure distribution is more efficient[25]. In this paper, we straightly use the pressure distribution[25]  $\mathbf{p}$  described by set of Tactel  $p_i$ , and the different robotic position  $\mathbf{r}$  results in the corresponding pressure distribution  $\mathbf{p}(\mathbf{r})$ . The pressure distribution  $\mathbf{p}(\mathbf{r})$  is expressed as

$$\mathbf{p}(\mathbf{r}) = \begin{bmatrix} p_1 \\ p_2 \\ \vdots \\ p_n \end{bmatrix} = \begin{bmatrix} p_1(\mathbf{r}) \\ p_2(\mathbf{r}) \\ \vdots \\ p_n(\mathbf{r}) \end{bmatrix} \in \mathbb{R}^n, \quad (1)$$

$$\mathbf{r} = \begin{bmatrix} r_1 \\ r_2 \\ \vdots \\ r_m \end{bmatrix} \in \mathbb{R}^m,$$

where  $n$  is the quantities of the tactels, and  $m$  is the degrees of freedom on the robot. And then, we differentiate the pressure distribution  $\mathbf{p}(\mathbf{r})$  expressed as

$$\dot{\mathbf{p}} = \mathbf{J}_t \dot{\mathbf{r}}, \quad (2)$$

where  $\mathbf{J}_t \in \mathbb{R}^{n \times m}$  is the tactile Jacobian that connects the time variation of pressure distribution  $\dot{\mathbf{p}}$  to the robotic velocity  $\dot{\mathbf{r}}$ . For tactile servo, the robotic velocity is the input for controlling a robot, and the principle shows in (3)

$$\dot{\mathbf{r}} = \mathbf{J}_t^\dagger \dot{\mathbf{p}}. \quad (3)$$

Meanwhile, we also have to estimate a tactile Jacobian  $\hat{\mathbf{J}}_t$  to satisfy (2), and the pseudo tactile Jacobian  $\hat{\mathbf{J}}_t^\dagger$  satisfies (3).

For robot control of tactile servo, the PI controller[26] was adopted in this study. The control scheme presents in Fig.3, and the control law is described by

$$\mathbf{u} = \mathbf{K} \hat{\mathbf{J}}_t^\dagger (\mathbf{e} + \frac{1}{T_i} \int \mathbf{e} dt), \quad (4)$$

$$\mathbf{e} = \mathbf{p}_{des} - \mathbf{p}_{cur}.$$

#### B. Dynamic Tactile Jacobian Estimator

In this study, the algorithm about the estimation of visual Jacobian [27] was adapted for dynamic tactile Jacobian estimator. From (2), we obtain the velocity relationship between pressure and robot motion, and (2) can be discretized with sampling  $T$  of tactile sensing array denoted by

$$\mathbf{p}(k+1) = \mathbf{p}(k) + \mathbf{J}_t(k) \mathbf{u}(k), \quad (5)$$

$$\mathbf{u}(k) = T \dot{\mathbf{r}}(k),$$

where  $\mathbf{u}$  is the information of robot in  $k$ -th sampling of tactile sensor, and  $\mathbf{J}_t$  is tactile Jacobian. In  $(k+1)$ th sampling, we have

$$\mathbf{p}(k+2) = \mathbf{p}(k+1) + \mathbf{J}_t(k+1) \mathbf{u}(k+1). \quad (6)$$

In renewing tactile Jacobian, we calculate each row vector of tactile Jacobian instead of whole tactile Jacobian at once.

$\mathbf{j}_{t,i}^\top$  means the  $i$ -th row vector of  $\mathbf{J}_t$ , and  $\mathbf{j}_{t,i}^\top$  can be obtained by

$$\begin{aligned} & \{\mathbf{j}_{t,i}^\top(k+1) - \mathbf{j}_{t,i}^\top(k)\}\mathbf{u}(k+1) = \\ & \{\mathbf{p}(k+2) - \mathbf{p}(k+1) - \mathbf{J}_t(k)\mathbf{u}(k+1)\}_i, \end{aligned} \quad (7)$$

where

$$\begin{aligned} \mathbf{j}_{t,i}^\top(k+1)\mathbf{u}(k+1) &= \{\mathbf{p}(k+2) - \mathbf{p}(k+1)\}_i, \\ \mathbf{j}_{t,i}^\top(k)\mathbf{u}(k+1) &= \{\mathbf{J}_t(k)\mathbf{u}(k+1)\}_i. \end{aligned} \quad (8)$$

Thus, in order to obtain  $\mathbf{j}_{t,i}^\top$ , we use a weighted matrix  $\mathbf{W}$  to minimize the change of rate of solution of (7)[28][29]. We have the estimated tactile Jacobian  $\hat{\mathbf{j}}_{t,i}^\top$  that can satisfy (7) obtained by

$$\begin{aligned} \hat{\mathbf{j}}_{t,i}(k+1) - \hat{\mathbf{j}}_{t,i}(k) = \\ \frac{\{\mathbf{p}(k+2) - \mathbf{p}(k+1) - \mathbf{J}_t(k)\mathbf{u}(k+1)\}_i}{\mathbf{u}^\top(k+1)\mathbf{W}(k+1)\mathbf{u}(k+1)}\mathbf{W}(k+1)\mathbf{u}(k+1). \end{aligned} \quad (9)$$

Equation (9) describes the way how to obtain the next tactile Jacobian, and we know the value from observation  $\mathbf{p}(k+2)$  is necessary. However, it is impossible to obtain it in the real world, so extrapolation method is utilized to estimate the tactile Jacobian  $\mathbf{J}_t$  to solve the problem of the observing  $\mathbf{p}(k+2)$ . Therefore, (9) is modified as

$$\begin{aligned} \hat{\mathbf{j}}_{t,i}(k+1) - \hat{\mathbf{j}}_{t,i}(k) = \\ \frac{\{\mathbf{p}(k+1) - \mathbf{p}(k) - \mathbf{J}_t(k)\mathbf{u}(k)\}_i}{\mathbf{u}^\top(k)\mathbf{W}(k)\mathbf{u}(k)}\mathbf{W}(k)\mathbf{u}(k). \end{aligned} \quad (10)$$

In principle, we are able to obtain the tactile Jacobian  $\hat{\mathbf{J}}_t$ , and when  $\|\mathbf{u}\| = 0$ ,  $\|\{\mathbf{p}(k+1) - \mathbf{p}(k) - \hat{\mathbf{J}}_t(k)\mathbf{u}(k)\}_i\| \rightarrow 0$  in proper convergence speed. Therefore, the right side of (10) is not divergent.

However, in a real system, the right side of (10) is definitely divergent due to the disturbances in real world. In order to reduce the influence from the disturbances, an oblivion parameter  $\rho$ , which is a positive number between 0 and 1, is applied on (10). Therefore, (10) is modified as

$$\begin{aligned} \hat{\mathbf{j}}_{t,i}(k+1) - \hat{\mathbf{j}}_{t,i}(k) = \\ \frac{\{\mathbf{p}(k+1) - \mathbf{p}(k) - \mathbf{J}_t(k)\mathbf{u}(k)\}_i}{\rho + \mathbf{u}^\top(k)\mathbf{W}(k)\mathbf{u}(k)}\mathbf{W}(k)\mathbf{u}(k). \end{aligned} \quad (11)$$

The weighted matrix plays a critical role for solving the proper tactile Jacobian. It can be estimated by means of WLS (Weighted Least Square) method, and it is described by

$$\begin{aligned} \mathbf{W}(k) = \\ \frac{1}{\rho} \left\{ \mathbf{W}(k-1) - \frac{\mathbf{W}(k-1)\mathbf{u}^\top(k-1)\mathbf{W}(k-1)\mathbf{u}(k-1)}{\rho + \mathbf{u}^\top(k-1)\mathbf{W}(k-1)\mathbf{u}(k-1)} \right\}. \end{aligned} \quad (12)$$

The process for estimating the tactile Jacobian  $\mathbf{J}_t$  has already been described above, and the solutions for reducing the influence from noisy is also presented; however, we still need the method to estimate the initial tactile Jacobian in the first stage of first contacting.

### C. Initial tactile Jacobian

In principle, when a robot has a displacement, the acquirement of robotic displacement  $\Delta\mathbf{r}$  and the variation of pressure distribution  $\Delta\mathbf{p}$  is available described as

$$\begin{aligned} \Delta\mathbf{r} &= \mathbf{r}(k+1) - \mathbf{r}(k), \\ \Delta\mathbf{p} &= \mathbf{p}(k+1) - \mathbf{p}(k), \end{aligned} \quad (13)$$

where  $k$  is the order in sampling period of the tactile sensing system. We have the relationship between  $\Delta\mathbf{p}$  and  $\Delta\mathbf{r}$  expressed as

$$\Delta\mathbf{p} = \mathbf{J}_t\Delta\mathbf{r}, \quad (14)$$

where  $\mathbf{J}_t \in \mathbb{R}^{n \times m}$  is tactile Jacobian [30]. Equation (14) can be described in detail as

$$\begin{bmatrix} \Delta p_1 \\ \Delta p_2 \\ \vdots \\ \Delta p_n \end{bmatrix} = \begin{bmatrix} j_{11} & j_{12} & \dots & j_{1m} \\ j_{21} & j_{22} & \dots & j_{2m} \\ \vdots & \vdots & \ddots & \vdots \\ j_{n1} & j_{n2} & \dots & j_{nm} \end{bmatrix} \begin{bmatrix} \Delta r_1 \\ \Delta r_2 \\ \vdots \\ \Delta r_m \end{bmatrix}, \quad (15)$$

and the variation of each tactel is expressed as

$$\begin{aligned} \Delta p_i &= j_{i1}\Delta r_1 + j_{i2}\Delta r_2 + \dots + j_{im}\Delta r_m \\ &= \sum_{j=1}^m \Delta r_j j_{ij} \\ &= \Delta\mathbf{r}^\top \mathbf{j}_i, \end{aligned} \quad (16)$$

where  $\mathbf{j}_i = [j_{i1}, j_{i2}, \dots, j_{im}] \in \mathbb{R}^m$  is the  $i$ -th column of tactile Jacobian  $\mathbf{J}_t$ .

According to (16),  $\mathbf{j}_i$  can be estimated by means of the different displacements and the corresponding variations of tactel by linear regression model [30]. Equation (16) can be written as

$$\Delta p_i = \Delta\mathbf{r}^\top \mathbf{j}_i + \varepsilon_i, \quad (17)$$

where  $\varepsilon_i$  is the deviation. And the minimum numbers of set of the displacement and variation is  $m$ . Thus, the simultaneous equation for obtaining  $\mathbf{j}_i$  is expressed as

$$\begin{cases} \Delta p_{i,1} = \Delta\mathbf{r}_1^\top \mathbf{j}_i + \varepsilon_{i,1}, \\ \Delta p_{i,2} = \Delta\mathbf{r}_2^\top \mathbf{j}_i + \varepsilon_{i,2}, \\ \vdots \\ \Delta p_{i,m} = \Delta\mathbf{r}_m^\top \mathbf{j}_i + \varepsilon_{i,m}. \end{cases} \quad (18)$$

By least squares method,  $\mathbf{j}_i$  can be estimated, and  $\varepsilon_i$  is regulated to zero.

The tactile Jacobian  $\mathbf{J}_t$  consists of several  $\mathbf{j}_i$ , and can be obtained by estimating  $\mathbf{j}_i$  simultaneously. Equation (18) is

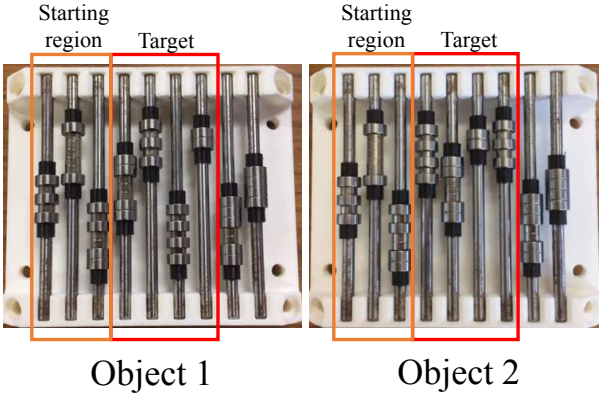


Fig. 4. Objects: the shape is similar to an abacus. Each object has a different pattern on its surface, respectively.

expanded as

$$\begin{aligned} \mathbf{P} &= \mathbf{R} \mathbf{J}_t^\top, \\ \mathbf{P} &= \begin{bmatrix} \Delta p_{1,1} & \Delta p_{2,1} & \dots & \Delta p_{n,1} \\ \Delta p_{1,2} & \Delta p_{2,2} & \dots & \Delta p_{n,2} \\ \vdots & \vdots & \dots & \vdots \\ \Delta p_{1,N} & \Delta p_{2,N} & \dots & \Delta p_{n,N} \end{bmatrix}, \\ \mathbf{R} &= \begin{bmatrix} \Delta r_{1,1} & \Delta r_{2,1} & \dots & \Delta r_{m,1} \\ \Delta r_{1,2} & \Delta r_{2,2} & \dots & \Delta r_{m,2} \\ \vdots & \vdots & \dots & \vdots \\ \Delta r_{1,N} & \Delta r_{2,N} & \dots & \Delta r_{m,N} \end{bmatrix}, \end{aligned} \quad (19)$$

where  $N$  cannot be less than  $m$ . From (19), the solution of inverse tactile Jacobian  $\mathbf{J}_t^\top$  is obtained by solving

$$\mathbf{J}_t^\top = \mathbf{R}^\dagger \mathbf{P}. \quad (20)$$

Thus  $\mathbf{J}_t$  is determined by transposing  $\mathbf{J}_t^\top$ . In (20),  $\mathbf{R}$  is usually not a square matrix.  $\mathbf{R}^\dagger$ , which is pseudo inverse matrix, is used instead of  $\mathbf{R}^{-1}$ .

#### IV. EXPERIMENTAL EVALUATION

##### A. Description of The Experiments

The conventional tactile Jacobian needs a large amount of data, such as pressure distribution and robot position, to be calculated by least squares methods. Moreover, the target for the conventional tactile Jacobian was only chosen in the data. However, the dynamic tactile Jacobian estimator just only needs an initial tactile Jacobian for the starting movement and the description of the desired pressure distribution to attain the target. According to the characteristics above, we utilized the objects which have the abacus-like appearance (see Fig.4), and the patterns in the starting region are identical, so the initial tactile Jacobian of each object is the same. The tactile Jacobian was only estimated once for the starting movement, which is different from the necessary of dull and repetitive estimation every time for the conventional tactile Jacobian to adjust to the different surface.

We use the starting region to acquire the displacement of the robot motions and their corresponding difference of the

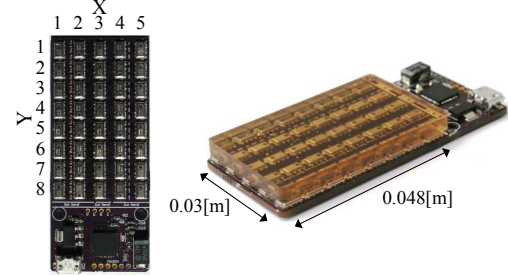


Fig. 5. Takkarray[31][32] is a tactile sensing array, which is composed of 40 sensing elements by MEMS barometer chips. The arrangement of the sensing area is a rectangle.

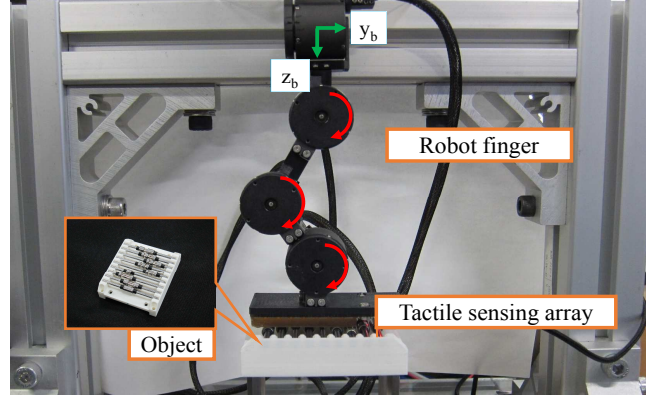


Fig. 6. Experimental system in this paper. The tactile sensor is mounted on the end-effector of the robot composed of 3 actuators. The robot can move on the surface of the object along the  $y$ -direction,  $z$ -direction, and rotate in  $x$ -orientation.

pressure distribution, and then the initial tactile Jacobian can be obtained. Then, while the robot is moving, the pressure distributions are obtained each sampling time. These series of pressure distributions are adopted to be the set of desired pressure distribution and each pressure distribution is called a step and numbered in a sequence, such as step 1, step 2, ..., etc.

During the experiment, the observed pressure distribution should match to each desired step. Only if the current desired step match, the desired pressure distribution will switch to the next desired step. The experiment will not accomplish until all the steps match. Normalized cross-correlation (NCC) is utilized to be the criterion of matching the desired step and the observed pressure distribution. The result of NCC calls  $R_{NCC}$  in this paper [25], and the threshold of  $R_{NCC}$  sets as 0.9. Only if threshold is equal to or beyond the threshold, the current desired step will be successful.

##### B. Equipment and Preparation

We adopted Takkarray(see Fig.5) to be the tactile sensor for this paper, and three actuators manufactured by YASKAWA are in series to be the robot. Then, the Takkarray is mounted on the end of the robot to be the end-effector. The whole system shown in Fig.?? is three degrees of freedom that the robot can operate in  $y$ -direction,  $z$ -direction, and  $x$ -orientation, and the objects for the experiments present in Fig.4.

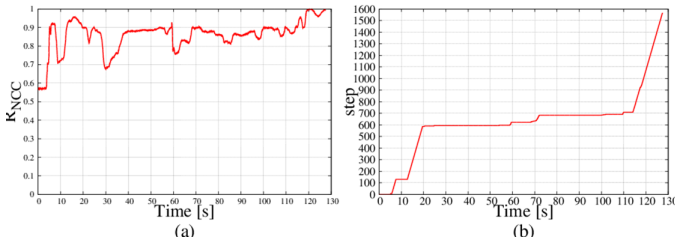


Fig. 7. Performance on object 1. (a) presents the similarity between the desired and observed pressure distribution by  $R_{NCC}$ . The higher the value is, the much more similar they are. (b) the result depicts the achievement by step. If  $R_{NCC}$  is greater than or equal to the threshold 0.9. The step will increase 1 until all desired steps are attained.

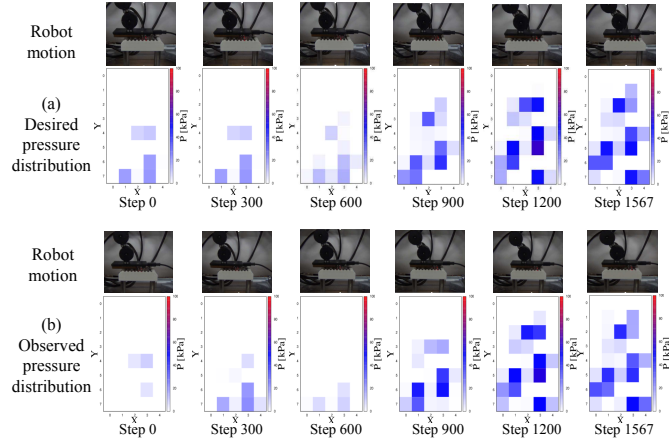


Fig. 8. Results of pressure distribution and robot motion in the specified steps for object 1. (a) The top results depict the desired steps and robot motions. (b) The bottom presents the experimental results including the observed pressure distribution and the robot motion.

Before experimenting, we have to acquire the initial tactile Jacobian in the starting region at first. We adopted the displacement of robot motion in the y-direction and the difference of pressure distribution to calculate the initial tactile Jacobian. Because the same patterns of the starting region on object 1 and object 2 result in the identical initial tactile Jacobian, the initial tactile Jacobian was only calculated once. And then we acquired a time-series of desired pressure distribution in y movement to be the target.

### C. Results of Experiments

Before the tactile servo using dynamic tactile Jacobian estimator was carried on, the desired set of pressure distribution should be obtained at first. The desired pressure distributions for two objects presents in Fig.8(a) and 10(a). The pressure distribution of object 1 and object 2 in step 0 and step 300 are the same, respectively due to the time difference in sensor recording and robot operating. But it was not a problem for being a desired pressure distribution.

$R_{NCC}$  evaluated the performance of the object with pattern 1, and Fig.7(a) shows the results. Fig.7(b) presents the completion of the total desired steps. The numbers of the desired steps and completed steps are 1567 and 1567, respectively. All the desired pressure distribution matches. In the experiment with

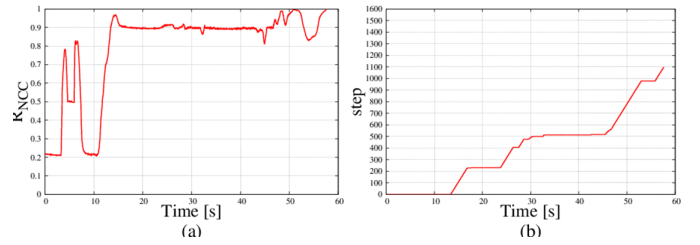


Fig. 9. Performance on object 2. (a) presents the similarity between the desired and observed pressure distribution by  $R_{NCC}$ . The higher the value is, the much more similar they are. (b) the result depicts the achievement by step. If  $R_{NCC}$  is greater than or equal to the threshold 0.9. The step will increase 1 until all desired steps are attained.

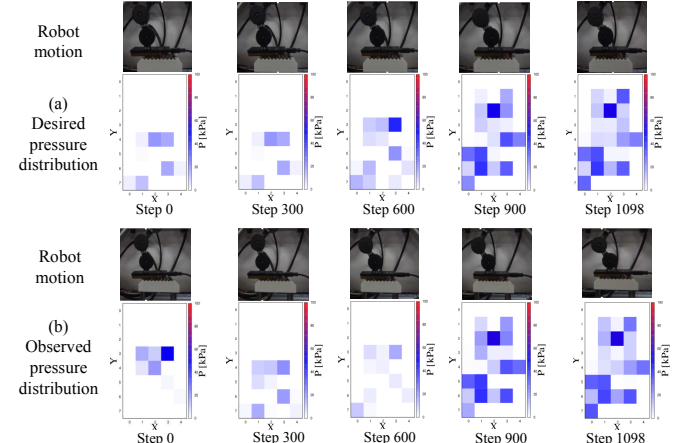


Fig. 10. Results of pressure distribution and robot motion in the specified steps for object 2. (a) The top depicts the desired steps and robot motions. (b) The bottom presents the experimental results including the observed pressure distribution and the robot motion.

the pattern 1, the actual results show in Fig.8(b). Tactile servo could execute by the dynamic tactile Jacobian estimator.

For the object with pattern 2, Fig.9(a) depicts the result of  $R_{NCC}$ . The completion of the total desired steps presents in Fig.9(b), and the numbers for the desired steps and completed steps are 1098 and 1098, respectively. All the desired pressure distribution also matches. The actual results of pressure distribution and the robot motion shows in Fig.10.

The validation with two different objects were both successful for the proposed method. In the experiments, the robot started from the starting region. The starting region of each object has the same pattern; namely, the initial tactile Jacobian is identical for each object. Then, the tactile servo with the dynamic tactile Jacobian estimator matches the all desired steps in the final. It means if the starting area is the same, the proposed method can be used on any surface for a robot to contact without prior information or data for the tactile Jacobian.

The other methods of calculating the tactile Jacobian for tactile servo have to collect the amount of the data about the tactile information and the corresponding robot motion in advance. Consequently, the tactile Jacobian is regular, and the time for preparation is longer than the proposed method in this paper. Besides, due to the regular tactile Jacobian, the tactile

servo can only operate in the range which is used to calculate its tactile Jacobian. So the proposed method is much more flexible comparing to the other methods.

#### D. Discussion and Future works

This research attempted to confirm the feasibility of the tactile servo with the dynamic tactile Jacobian estimator, and experimental results have been presented in the figures above. Finally, the feasibility of the proposed method was confirmed, and final performance conforms to the purpose mentioned in the beginning.

However, performance time is another critical issue for this proposed method. We can learn performance time from Fig.7 and Fig.9, respectively. To complete the experiment, both of them take more than 50 sec. In this paper, we provided a method to calculate the tactile Jacobian for the next movement of the robot. In the future, we may be able to provide several different methods to calculate the tactile Jacobian. By training, the tactile servo can quickly find out the proper method for calculating tactile Jacobian to increase the performance on performance time.

#### V. CONCLUSION

In this paper, we have demonstrated the performance of the tactile servo using dynamic tactile Jacobian estimator. The tactile Jacobian is dynamic, so the tactile servo with the proposed method is much more flexible than the conventional tactile Jacobian. The robot adopted this proposed method can easily touch and contact any surface of an object or operate the object, even though the information on the surface of the object is unknown. We believe our method can facilitate the advanced issues in robot manipulation or the service robots which need to interact with their surroundings.

#### ACKNOWLEDGMENT

This work was supported by JSPS KAKENHI, Grant Number 16H04292.

#### REFERENCES

- [1] C. Jiang, Y. Nakatomi, and S. Ueno, S. Optimal control of holding motion by nonprehensile two-cooperative-arm robot. In *Mathematical Problems in Engineering*, 2016.
- [2] H. Iwata, and S. Sugano. (2009, May). Design of human symbiotic robot TWENDY-ONE. In *Proc. IEEE Int. Conf. on ICRA*, pages 580-586, 2009.
- [3] H. Iwata, and S. Sugano. (2009, May). Design of human symbiotic robot TWENDY-ONE. In *IEEE Int. Conf. on ICRA*, pages 580-586, 2009.
- [4] M. C. Koval, N. S. Pollard, and S. S. Srinivasa. (2015). Pose estimation for planar contact manipulation with manifold particle filters. In *The International Journal of Robotics Research*, 34(7), pages 922-945, 2015
- [5] M. Ding, R. Ikeura, T. Mukai, H. Nagashima, S. Hirano, K. Matsuo, and S. Hosoe. Comfort estimation during lift-up using nursing-care robot RIBA. In *Proc. IEEE Int. Conf. on ICIES*, pages 225-230, 2012.
- [6] M. Ding, R. Ikeura, Y. Mori, T. Mukai, and S. Hosoe. Lift-up motion generation of nursing-care assistant robot based on human muscle force and body softness estimation. In *Proc. IEEE/ASME Int. Conf. on AIM*, pages 1302-1307, 2014.
- [7] T. Mukai, S. Hirano, H. Nakashima, Y. Kato, Y. Sakaida, S. Guo, and S. Hosoe. Development of a nursing-care assistant robot RIBA that can lift a human in its arms. In *Proc. IEEE/RSJ Int. Conf. on IROS*, pages 5996-6001, 2010.
- [8] T. Mukai, S. Hirano, M. Yoshida, H. Nakashima, S. Guo, and Y. Hayakawa. Tactile-based motion adjustment for the nursing-care assistant robot RIBA. In *Proc. IEEE Int. Conf. on ICRA*, pages 5435-5441, 2011.
- [9] T. Mukai, S. Hirano, M. Yoshida, H. Nakashima, S. Guo, and Y. Hayakawa. Whole-body contact manipulation using tactile information for the nursing-care assistant robot riba. In *Proc. IEEE/RSJ Int. Conf. on IROS*, pages 2445-2451, 2011.
- [10] H. Y. Chow and R. Chung. Obstacle avoidance of legged robot without 3D reconstruction of the surroundings. In Proceedings 2000 ICRA. Millennium Conference. IEEE International Conference on Robotics and Automation. Symposia Proceedings (Cat. No. 00CH37065) (Vol. 3, pp. 2316-2321). IEEE.
- [11] X. Nan-Feng, and S. Nahavandi. Visual feedback control of a robot in an unknown environment (learning control using neural networks). *The International Journal of Advanced Manufacturing Technology*, 24(7-8), 509-516.
- [12] P. K. Allen, A. Timcenko, B. Yoshimi, and P. Michelman, Automated tracking and grasping of a moving object with a robotic hand-eye system. In *IEEE Transactions on Robotics and Automation*, 9(2), 152-165, 1993.
- [13] C. Schurmann, R. Haschke, and H. Ritter. A modular high-speed tactile sensor for human manipulation research. In *IEEE World Haptics Conference* pages 339-344, 2011.
- [14] K. J. Overton, and T. Williams. Tactile Sensation for Robots. In *IJCAI* pages 791-795, 1981.
- [15] T. Nagatani, A. Noda, and S. Hirai. What can be inferred from a tactile arrayed sensor in autonomous in-hand manipulation? In *Proc. IEEE Int. Conf. on CASE*, pages 461-468, 2012.
- [16] H. Zhang, and N. N. Chen. Control of contact via tactile sensing. *IEEE Transactions on Robotics and Automation*, 16(5): 482-495, 2000.
- [17] N. Chen, H. Zhang, and R. Rink. Tactile sensing of point contact. In *Proc. IEEE Int. Conf. on IROS* pages 574-579, 1995.
- [18] C. Muthukrishnan, D. Smith, D. Myers, J. Rebman, and A. Koivo. Edge detection in tactile images. In *Proc. IEEE Int. Conf. on ICRA*, Vol. 4, pages 1500-1505, 1987.
- [19] H. Maekawa, K. Tanie, and K. Komoriya. Manipulation of an unknown object by multifingered hand with rolling contact using tactile feedback. *IEEE Transactions of the Society of Instrument and Control Engineers*, 31(9): 1462-1470, 1995.
- [20] N. Houshangi, A. J. Koivo. (1989, November). Tactile sensor control for robotic manipulations. In *Proc. IEEE Int. Conf. on SMC*, pages 1258-1259, 1989.
- [21] P. Sikka, H. Zhang, and S. Sutphen. Tactile servo: Control of touch-driven robot motion. In *Experimental Robotics III*, pages 219-233, Springer, Berlin, Heidelberg, 1994.
- [22] Q. Li, C. Schurmann, R. Haschke, and H. Ritter. A control framework for tactile servoing. In *Robotics: Science and Systems*, 2013.
- [23] N. Chen, H. Zhang, and R. Rink. Edge tracking using tactile servo. In *Proc. IEEE/RSJ Int. Conf. on IROS*, pages 84-89, 1995.
- [24] N. Chen, H. Zhang, and R. E. Rink. Touch-driven robot control using a tactile Jacobian. In *Proc. IEEE Int. Conf. on ICRA*, pages 1737-1742, 1997.
- [25] C. T. Wen, J. Kinugawa, S. Arai, and K. Kosuge. (2019, August). Tactile Servo Based on Pressure Distribution. In *IEEE Int. Conf. on ICMA*, pages 868-873, 2019
- [26] R. Garrido, A. Soria, and M. Trujano. Visual PID control of a redundant parallel robot. In *Proc. IEEE Int. Conf. on Electrical Engineering, Computing Science and Automatic Control*, pages 91-96, 2018.
- [27] K. Hosoda, and M. Asada. Versatile visual servoing without knowledge of true jacobian. In *Proc. IEEE/RSJ Int. Conf. on IROS*, Vol. 1 pages 186-193, 1994
- [28] L. Ljung. System identification. Wiley Encyclopedia of Electrical and Electronics Engineering, 2001
- [29] M. Bartholomew-Biggs. Nonlinear optimization with engineering applications (Vol. 19). Springer Science and Business Media, 2008
- [30] S. Weisberg. Applied linear regression (Vol. 528). John Wiley and Sons, 2005.
- [31] TakkTile. <http://www.takktile.com/documentation> (14, January, 2016)
- [32] Y. Tenzer, L. P. Jentoft, and R. D. Howe. Inexpensive and easily customized tactile array sensors using MEMS barometers chips. *IEEE Robot. Autom. Mag*, 21(3): 89-95, 2014.